FISEVIER

Contents lists available at ScienceDirect

### **Quaternary Science Reviews**

journal homepage: www.elsevier.com/locate/quascirev



## Abrupt Holocene climate change and potential response to solar forcing in western Canada

Daniel G. Gavin  $^{a,*}$ , Andrew C.G. Henderson  $^{a,1}$ , Karlyn S. Westover  $^b$ , Sherilyn C. Fritz  $^b$ , Ian R. Walker  $^c$ , Melanie J. Leng  $^{d,e}$ , Feng Sheng Hu  $^{a,f}$ 

- <sup>a</sup> Department of Plant Biology, University of Illinois at Urbana-Champaign, 505 South Goodwin Avenue, Urbana, IL 61801, USA
- <sup>b</sup> Department of Earth and Atmospheric Sciences, University of Nebraska, Lincoln, NE 68588-0340, USA
- <sup>c</sup>Department of Biology, University of British Columbia, Okanagan, Kelowna, BC V1V 1V7, Canada
- <sup>d</sup> NERC Isotope Geosciences Laboratory, British Geological Survey, Keyworth, Nottingham NG12 5GG, UK
- <sup>e</sup> School of Geography, University of Nottingham, Nottingham NG7 2RD, UK
- Department of Geology, University of Illinois at Urbana-Champaign, Natural History Building, Urbana, IL 61801, USA

#### ARTICLE INFO

# Article history: Received 13 August 2010 Received in revised form 28 February 2011 Accepted 3 March 2011 Available online 29 March 2011

Keywords:
Abrupt climate change
Atmospheric circulation
Biogenic silica
British Columbia
Diatoms
Solar forcing

#### ABSTRACT

Several abrupt climate events during the Holocene, including the widely documented oscillation at 8.2 thousand years before present (ka), are attributed to changes in the North Atlantic thermohaline circulation. Additional mechanisms, such as interactions between atmospheric circulation, ice-sheet dynamics, and the influence of solar irradiance, also have been proposed to explain abrupt climatic events, but evidence remains elusive. This study presents evidence from multi-proxy analyses on the Holocene sediments of Eleanor Lake, interior British Columbia. Climatic inferences from our decadalresolution record of biogenic silica (BSi) abundance are supported by changes in diatom and pollen assemblages from the same core and correlations with existing regional climate records. The BSi record reveals abrupt and persistent climatic shifts at 10.2, 9.3, and 8.5 ka, the latter two of which are coeval with major collapses of the Laurentide Ice Sheet. The record also reveals a short-term cooling at 8.2 ka that is distinct from the 8.5 ka event and similar in magnitude to several other late-Holocene coolings. BSi is correlated with solar-irradiance indices (r = 0.43 - 0.61), but the correlation is opposite in sign to that expected from direct solar forcing and weakens after 8 ka. Possible mechanisms causing the abrupt and persistent climate changes of the early Holocene include 1) sudden losses of ice and proglacial lake extent, causing a shift in the meridional structure of atmospheric circulation, 2) a possible link between solar minima and El Niño-like conditions that are correlated with warm spring temperature in interior British Columbia, and 3) the influence of solar irradiance variability on the position of the polar jet, possibly via effects on the strength of the glacial anticyclone.

© 2011 Elsevier Ltd. All rights reserved.

#### 1. Introduction

Understanding the mechanisms of abrupt climate change requires identification of such events in high-resolution paleoclimate records and associating them with forcing factors that may have pushed the climate system past a threshold (Alley et al., 2003; Denton et al., 2010). Apart from the events attributable to

thermohaline circulation shutdown in the North Atlantic during deglaciation (e.g., Kleiven et al., 2008), evidence of abrupt and long-lasting (>several centuries) climate change events during the Holocene with plausible alternative mechanisms remains scarce in many regions. However, several mechanisms have been proposed, including abrupt shifts in the jet stream upstream of ice sheets associated with rapid deglaciation (Wunsch, 2006) and solar variability as a modulator of centennial-scale climatic fluctuations (Björck et al., 2001; Bond et al., 2001; Hu et al., 2003).

The scattered evidence of abrupt Holocene climate change nodoubt reflects the paucity of high-resolution records of sensitive climate proxies in regions that experienced abrupt events. Candidate regions for detecting abrupt Holocene climate events include transitions between climatic regimes and air-mass dominance (Kirby et al., 2002). One such region is eastern British Columbia in

Abbreviations: ka, thousands of calendar years before present; BSi, biogenic silica.

<sup>\*</sup> Corresponding author. Present address: Department of Geography, University of Oregon, Eugene, OR 97403-1251, USA. Tel.: +1 541 346 5787; fax: +1 541 346 2067. E-mail address: dgavin@uoregon.edu (D.G. Gavin).

<sup>&</sup>lt;sup>1</sup> Present address: School of Geographical & Earth Sciences, University of Glasgow, East Quadrangle, University Avenue, Glasgow G12 8QQ, UK.

western Canada, where winter onshore flow collides with polar air masses, producing abundant snowfall, and where summer convective rainfall also is frequent. In this study, we analyzed sediments from Eleanor Lake (Fig. 1; 52°7'N, 119°18'W; 677 m above sea level) in east-central British Columbia to infer patterns and drivers of Holocene climatic change. While the regional climate may be sensitive to large-scale forcing, paleolimnological approaches to climate reconstruction present challenges because the year-round wet climate may result in little climatic sensitivity of the biogeochemistry of lake water or of the assemblages and productivity of the diatom flora (Battarbee, 2000). It is possible, however, that the cool summer climate and variable ice-off dates affect springtime water temperature, nutrient dynamics, diatom species assemblages, and productivity (Smol and Douglas, 2007). Here we infer Holocene climatic change in the Eleanor Lake area from a variety of sediment measurements, with a focus on the biogenic silica (BSi) content, diatom assemblages, and pollen assemblages. These inferences are compared with nearby independent temperature-sensitive climate proxy records. Furthermore, we compared the Eleanor Lake climate record with commonly used proxies of solar activity, as several recent studies have shown that millennial-scale climate fluctuations throughout the Holocene are correlated with ice-core and tree-ring proxies of solar activity (e.g., Björck et al., 2001; Bond et al., 2001; Hu et al., 2003; Marshall et al., 2007; Marchitto et al., 2010).

#### 2. Geomorphic and hydrologic setting

Eleanor Lake is a 9.5-ha, 19-m deep, kettle lake in the valley floor of the North Thompson River in the town of Blue River, British Columbia. The climate of the region is cool and moist, with an average July temperature of 16.3 °C and an average annual precipitation of 1002 mm, 30% of which falls as snow (Fig. 1). The bedrock is classified in the Shuswap Assemblage, dominated by

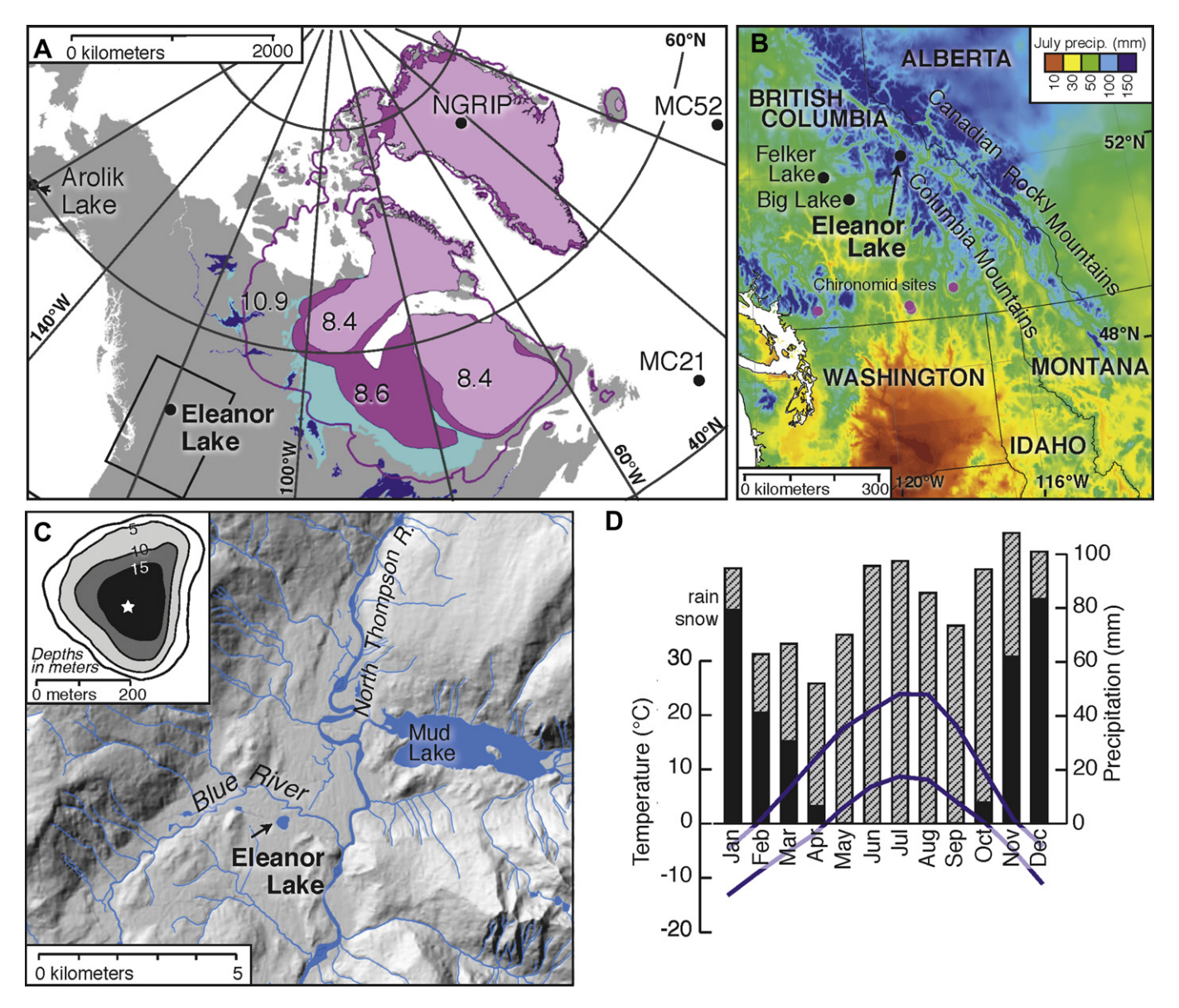


Fig. 1. Geographic setting of the study area. (A) The extent of the Laurentide Ice Sheet at three times (8.4 and 8.6 ka shown in magenta, and 10.9 ka shown by a line). Turquoise indicates proglacial lakes at 8.6 ka, and blue indicates modern large lakes (Dyke et al., 2003). Comparison sites in Alaska, Greenland, and the North Atlantic (ice-rafted debris record) also are shown. (B) July precipitation and locations of lake sites mentioned in the text. (C) Shaded-relief map of the mountainous landscape and bathymetric map showing the core site location within the 9.5 ha lake. (D) Monthly averages (1960–1999) of maximum and minimum temperature (blue lines) and precipitation (bars) for Eleanor Lake (Blue River, BC). (For interpretation of the references to colour in this figure legend, the reader is referred to the web version of this article.)

metamorphic rocks of quartzofeldspathic gneiss and biotite-quartz schist (Massey et al., 2005). The lake has no inflowing or outflowing streams and has a catchment of <5 ha, though delimiting the catchment is difficult due to its location on a low-relief glaciofluvial terrace. Springs occur at ca 4 m depth on the west side of the lake, suggesting that the lake exchanges water with the hyporheic flow of Blue River, located 150 m to the north. Late-successional forests in the region are composed of the mesophytic trees *Tsuga heterophylla* and *Thuja plicata*. Extensive seral forests are composed of *Pinus contorta*, *Pseudotsuga menziesii* and *Betula papyrifera*. *Picea engelmannii* x *glauca* and *Abies lasiocarpa* are abundant above 900 m, but also occur rarely near the lake.

#### 3. Materials and methods

#### 3.1. Core collection and chronology

Two parallel cores were obtained from the deepest location of the lake using a modified square-rod Livingstone piston corer from an anchored platform. Cores were extruded and wrapped in the field and split lengthwise in the laboratory. The upper-most 57-cm of sediment was obtained using a clear polycarbonate tube fitted with a piston. The surface-sediment core was sectioned into plastic bags at 1-cm intervals in the field. The chronology of the sediments is based on nine <sup>14</sup>C ages on plant macrofossils, three volcanic-tephra ages, and <sup>210</sup>Pb ages on the upper 27 cm of sediment. Calibration of <sup>14</sup>C ages to the calendar age scale was made using CALIB 5.0 (Stuiver and Reimer, 1993; Reimer et al., 2004). An age—depth model was constructed using a monotonic cubic spline. Before curve fitting, depths were adjusted to account for the thicknesses of tephras.

#### 3.2. Sediment chemical analyses

The organic content of the lake sediment was measured using loss-on-ignition (at 550 °C) on 85 samples, and organic C and organic N were measured using a UIC CHN analyzer on an additional 55 samples. The relative proportions of the major identified minerals were determined on 29 samples by x-ray diffraction with a Scintag — diffractometer following conventional procedures (Moore and Reynolds, 1997).

We measured BSi on 495 samples spaced at 1 to 2-cm intervals. BSi was extracted from ca 60 mg of freeze-dried sediment with 10%  $Na_2CO_3$ , dyed with molybdate blue, and measured with a spectro-photometer previously calibrated on a silica standard solution (modified from Mortlock and Froelich, 1989). BSi was then calculated as the percent biogenic  $SiO_2$  of the total dry weight. The 95% confidence interval of the BSi measurements, determined from 29 replicate samples, was  $\pm 4.6\%$  and this error did not vary with the absolute value of BSi or with the depth in the core.

In order to compare the Eleanor Lake BSi record to proxies of solar activity, we used the smoothed and detrended records of  $^{10}$ Be flux from the GRIP and GISP2 Greenland ice cores and the production rate of  $^{14}$ C computed from  $\Delta^{14}$ C of the tree-ring calibration curve (Bond et al., 2001; Reimer et al., 2004; Marchitto et al., 2010). These proxies were detrended to remove the potential effect of long-term fluctuations in the geomagnetic field on cosmogenic nuclide production (Marchitto et al., 2010). We smoothed and detrended the BSi record in the same manner to make it comparable to the solar proxies of Marchitto et al. (2010). Specifically, we used a running mean in a ca 100-year window on the raw observations, a linear detrend, interpolation to 50-year intervals, and then a high-pass filter at 1/1800 year $^{-1}$ . Testing the significance of the correlation between the BSi and solar proxies required a method that accounted for a temporal autocorrelation,

as such autocorrelation violates an assumption of parametric significance tests. We used a block bootstrap in which each bootstrap sample involved resampling (with replacement) the BSi time series in blocks of 150 years (i.e., three consecutive points of the 50-year resampled time series). The bootstrap distribution of the correlation coefficient was calculated using 999 bootstrap samples of the time series. A two-tailed significance test was assessed using the bootstrap distribution.

#### 3.3. Diatom and pollen analyses

Diatom samples (n=117) were treated with 10% hydrochloric acid and cold 35% hydrogen peroxide to remove carbonates and organic matter, respectively (Battarbee et al., 2001). Diatom samples were mounted on glass slides with Zrax and examined at  $1000 \times 1000$  magnification. A minimum of 300 valves was identified per sample. Taxonomic identifications were made with reference to several sources (Patrick and Reimer, 1975; Krammer and Lange-Bertalot, 1991; Cumming et al., 1995). A tally of undifferentiated chrysophyte cysts encountered during the diatom count also was made.

Pollen samples (n = 69) of 0.5—1 cm<sup>3</sup> were chemically processed using standard base, acid, and acetolysis treatments (Faegri and Iversen, 1992). Pollen samples were mounted on slides using Si oil and examined at  $400\times$  and  $1000\times$  magnification. A minimum of 350 terrestrial pollen grains was identified per sample. Taxonomic identifications were made using a reference collection and taxonomic keys (e.g., Faegri and Iversen, 1992).

#### 4. Results

#### 4.1. Sediment chronology and characteristics

The 682-cm sediment core is characterized as brown gyttja with microlaminations and black banding, three volcanic tephras, and in the basal 35 cm, alternating clay and organic sediment overlying coarse sand and gravel. The basal calibrated <sup>14</sup>C age of the core is 10.85 ka, and the sequence of <sup>14</sup>C dates shows no age reversals. However, one date from a marginal quantity of unidentifiable plant material fell out of line with neighboring dates and had a large standard deviation (Table 1). This date is not included in the age—depth model (Fig. 2). The <sup>210</sup>Pb concentrations fluctuate greatly in the upper 10 cm of sediment, consistent with a known history of recent anthropogenic pollution causing algal blooms followed by restoration efforts that would have reduced sedimentation rates (Table 2).

Multiple visual tie-points between two parallel cores permitted continuous sampling down-core at 1-cm intervals. Although the record is continuous, there is a distinct 46-cm core segment immediately following the airfall Mazama tephra that is heavily contaminated with redeposited tephra representing a 310-year period (estimated with our <sup>14</sup>C chronology; Fig. 2). This core segment was removed from subsequent analyses because the redeposited tephra greatly reduced % BSi. Overall, the robust chronology, along with the high deposition rate and minimal sediment mixing as evidenced by microlaminations, permitted the detection and dating of abrupt climatic events.

The sediments of Eleanor Lake are composed primarily of BSi and organic matter (Fig. 2). Diatom preservation was good to excellent throughout the core, suggesting little dissolution effects on the BSi record. Mineral content, comprised mainly of pyrite (40–60% of the major identified minerals), exceeds 25% of the sediment dry weight only at the core base and at depths of tephras. The occurrence of pyrite throughout the core suggests that the lake has been continuously deep and that the bottom water has remained anoxic.

**Table 1**14C dates and tephras from the Eleanor Lake sediment record. Terrestrial macrofossils were dated by accelerator mass spectrometry (AMS) at the Center for Accelerator Mass Spectrometry at Lawrence Livermore National Laboratory.

Lab Code (CAMS#) or tephra	Depth from sediment surface (cm) <sup>a</sup>	Dated material or reference for tephra	<sup>14</sup> C age	Calibrated age (median and $2\sigma$ range)
108931	73 (73)	Picea needle	$785 \pm 70$	710 (670–760)
114114	117 (117)	Betula cone scale	$1590 \pm 70$	1470 (1400-1550)
Bridge River tephra	156.5-157.5 (156.5)	Clague et al., 1995		2400
St. Helens Yn tephra	202-203 (201)	Foit et al., 2004		3640
108932	224 (222)	Picea needle	$3945\pm70$	4400 (4260-4520)
108933	256 (254)	Picea needle	$4750\pm70$	5510 (5329-5586)
114115	300 (298)	Leaf petiole	$6385 \pm 70$	7320 (7260-7418)
Mazama tephra	347-355 (345)	Zdanowicz et al., 1999		7627
114116	401 (391)	Leaf (Betula or Alnus)	$7760 \pm 90$	8530 (8430-8600)
114117	467 (457)	Leaf (Betula or Alnus)	$8360 \pm 70$	9390 (9300-9470)
114118 <sup>b</sup>	536 (526)	Fibrous plant material	$8530 \pm 180$	9520 (9300-9700)
114119	598 (588)	Leaf (Betula or Alnus)	$9020\pm70$	10,210 (10,170-10,240)
108934	672 (662)	Pinus needle	$9520 \pm 90$	10,850 (10,660-11,090)

<sup>&</sup>lt;sup>a</sup> Values in parentheses are depths corrected for tephra thicknesses.

#### 4.2. BSi, diatom, and pollen stratigraphy

From 10.6 to 10.2 ka, BSi (expressed as a percentage of dry weight) increased rapidly from ca 5% to nearly 50% (Fig. 3). BSi then

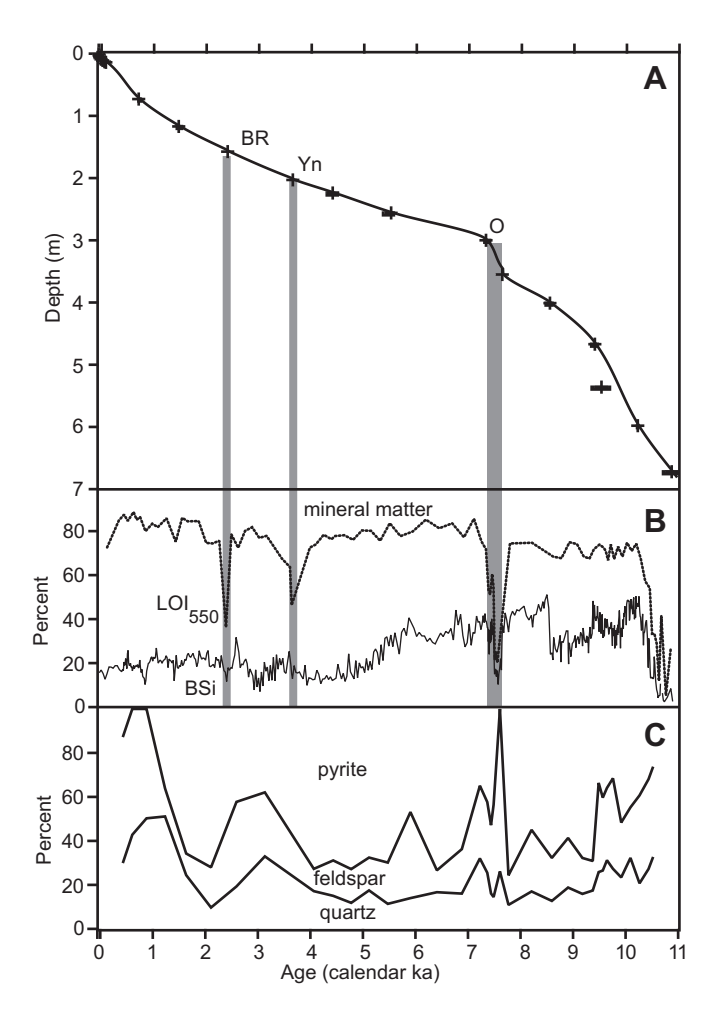


**Fig. 2.** (A) Age—depth relationship of the 6.8-m sediment core from Eleanor Lake. Crosses show the median of 10 calibrated AMS  $^{14}\mathrm{C}$  dates on macrofossils, the known ages of three tephras (O, BR, Yn), and  $^{210}\mathrm{Pb}$  age model of surface sediments. The  $2\sigma$  errors of  $^{14}\mathrm{C}$  dates are shown by horizontal bars. Gray vertical bars indicate sediments containing tephra, including a 310-year period of redeposited Mazama (O) tephra. (B) Stacked percentages of biogenic silica (BSi) and percent loss-on-ignition at 550 °C (LOl $_{550}$ ). LOI was analyzed at coarser intervals than BSi. (C) Stacked percentage graph of the major identified minerals determined by X-ray diffraction.

decreased slowly until 9.9 ka, then dropped to 32% and at 9.3 ka peaked again near 45%. After 9.3 ka, BSi decreased abruptly to 30%, and then decreased more slowly to 25% by 8.5 ka, when it increased abruptly to ca 50%. After 8.5 ka, BSi decreased briefly at 8.2 ka and then gradually to 35% until ca 6 ka. From 6 to 4.2 ka, BSi steadily decreased to 15%. After 4.2 ka BSi fluctuated between 10% and 30% with several distinct decadal-scale peaks and troughs.

In general, diatom assemblages (Fig. 3) fluctuated greatly with changing BSi. The initial increase in BSi was marked by a transition from a diverse benthic assemblage to a diverse planktonic assemblage dominated briefly by *Stephanodiscus minutulus*, which then transitioned to *Fragilaria crotonensis*. The 9.3 ka BSi peak was similar to the 10.2 ka peak with dominance by *S. minutulus* transitioning to dominance by *Fragilaria* spp. The 8.5 ka BSi peak was comprised mainly of *S. minutulus* and *Cyclotella bodanica* aff. *lemanica*. After 8.5 ka, a period of decreasing BSi was dominated by *C. bodanica* and also showed an increase in the chrysophyte cyst to diatom ratio. After 4.2 ka diatom assemblages were dominated by tychoplanktonic *Fragilaria capucina* except for a peak of *Cyclotella* spp. coincident with a BSi peak and a peak of benthic diatoms (*Pinnularia mesolepta*) during the last millennium.

The pollen assemblages are dominated by *Pinus*, representing locally and regionally dispersed *P. contorta* pollen (Fig. 4). Before 10.4 ka, during the period of rapidly increasing organic content, macrofossils indicate that *P. contorta* first colonized the area and *Pinus* pollen dominated (ca 97%) with minor amounts of *Alnus*. *Pinus* percentages declined until 9.3 ka while *Abies* cf. *lasiocarpa* 

**Table 2**<sup>210</sup>Pb determinations and age estimates from the surface sediments of Eleanor Lake. Values in bold were averaged to calculate background activities used in the age model. Estimated ages were determined by a constant-rate-of-supply (CRS) model.

Depth in sediment (cm)	Bulk density (g/cm³)	Activity (DPM/g)	Estimated age
0-1	0.0127	105.436	2002
2-3	0.0191	155.162	1998
4-5	0.0244	75.033	1994
6-7	0.0282	280.571	1973
8-9	0.0345	67.358	1947
10-11	0.0305	42.786	1916
12-13	0.0030	26.696	1880
13-14	0.0714	21.335	1855
14-15	0.0393	24.773	
16-17	0.0377	15.885	
18-19	0.0426	14.764	
20-21	0.0444	12.176	
22-23	0.0365	18.145	
24-25	0.0478	16.536	
25-26	0.0525	12.945	
26-27	0.0331	10.194	

<sup>&</sup>lt;sup>b</sup> Date rejected for chronology development.

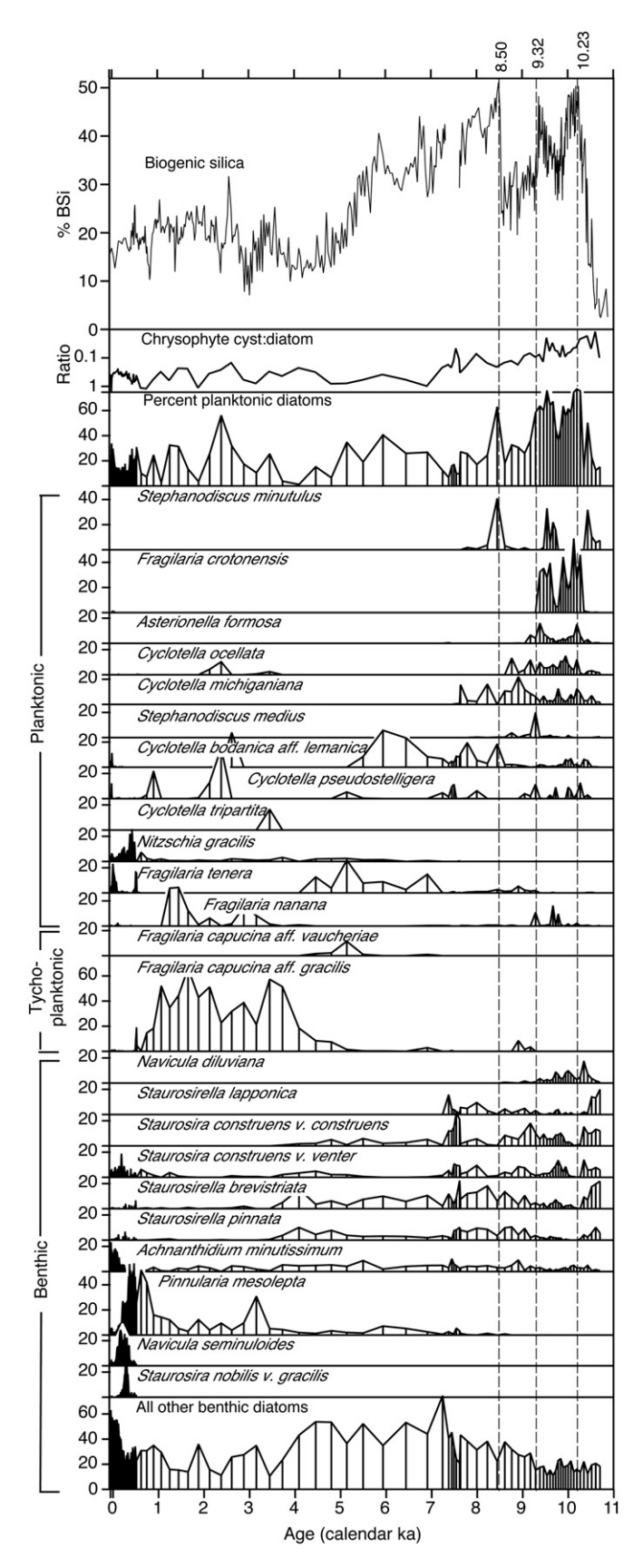


**Fig. 3.** The BSi and diatom record from Eleanor Lake. The vertical dashed lines indicate the three largest abrupt changes in the BSi record.

pollen increased to 10%, followed by *Betula* and *Picea*. *Betula* pollen, most likely *B. papyrifera* based on occasional seeds, decreased abruptly after 8.5 ka, when *Pinus* increased again followed by *Picea* (and the first appearance of *P. engelmannii* macrofossils) and *Pseudotsuga*. After the deposition of Mazama tephra at 7.6 ka, *Pinus*, *Picea* and *Abies* percentages remained steady while *Betula* and *Alnus* pollen declined into the late Holocene. *T. heterophylla* pollen became consistently present (>2%) at 4.5 ka and a *T. heterophylla* needle was found at 3.9 ka. Cupressaceae pollen, representing *T. plicata*, was consistently represented after ca 3 ka.

#### 5. Paleoclimatic interpretation of biogenic silica

#### 5.1. Multi-proxy evidence from Eleanor Lake

BSi and organic matter (estimated by loss-on-ignition) together comprise on average 75% of the sediment dry weight (Fig. 2), and their fractions are negatively correlated. Specifically, BSi has a strong negative correlation with % organic nitrogen (% ON) and % organic carbon (% OC) (r=-0.86 and -0.88, respectively; Fig 5). While fluctuations in one component (e.g., OC) affect the percent of the other component (e.g., BSi), we note that if computing % BSi and % OC relative to non-BSi mineral matter only (thus removing codependence of BSi and OC), these correlations are roughly halved but remain negative, despite the fact that a portion of the OC in the sediment is diatom-bound organic matter. Therefore, variable partitioning of aquatic productivity between siliceous and non-siliceous organisms must be invoked to explain the fluctuations in % BSi. This is supported by an average OC/ON ratio of 12.8 indicating a mostly aquatic origin of the organic matter (Meyers and Lallier-Vergas, 1999).

Expressing BSi and organic matter as accumulation rates (i.e.,  $mg\,cm^{-2}\,yr^{-1}$ ) may potentially overcome the issue of interdependence of percentage measures. However, BSi and organic matter accumulation rates parallel the total sedimentation rate over the Holocene to such a degree that any productivity signal in accumulation rates is likely overshadowed by basin-controlled sediment focusing. We suggest that the bathymetry of Eleanor Lake would have been more conical in shape during the early Holocene, thereby favoring sediment focusing and the observed high sedimentation rate at that time (Hilton, 1985). Thus, while BSi accumulation rates are a result of an unknown mixture of sediment focusing and BSi productivity, BSi expressed as a percent of dry weight is more simply a trade-off of BSi versus organic matter production. Several other factors, discussed below, support a climatic interpretation of % BSi.

BSi percentages are positively correlated with the percent of planktonic diatoms (r = 0.73; Fig 5D), indicating BSi is a proxy for the conditions suitable for spring planktonic diatom blooms. Such conditions occur following ice-out and prior to thermal stratification when physical mixing results in the upward transfer of nutrients from the hypolimnion. Periods of extended spring mixing, such as after an early ice-out due to winters with low snow cover and rapid spring warm-up (Bradbury, 1988; Interlandi et al., 1999) are likely to enhance planktonic diatom productivity. Eleanor Lake currently experiences heavy snowfall (423 cm annually) and cool summers (July mean temperature = 16.3 °C), both of which would limit planktonic diatom productivity via late ice-off and low growing-season temperature. Consistent with this interpretation is that chrysophyte cysts, known to be abundant in cool and oligotrophic conditions (Lotter et al., 1997), are negatively correlated with % BSi despite the fact that chrysophyte cysts also contribute to BSi (Fig. 5E).

The major peaks in BSi during the early Holocene are marked by a succession from *S. minutulus* to *F. crotonensis* and *Asterionella formosa*. *S. minutulus* blooms rapidly following ice out (Interlandi et al.,

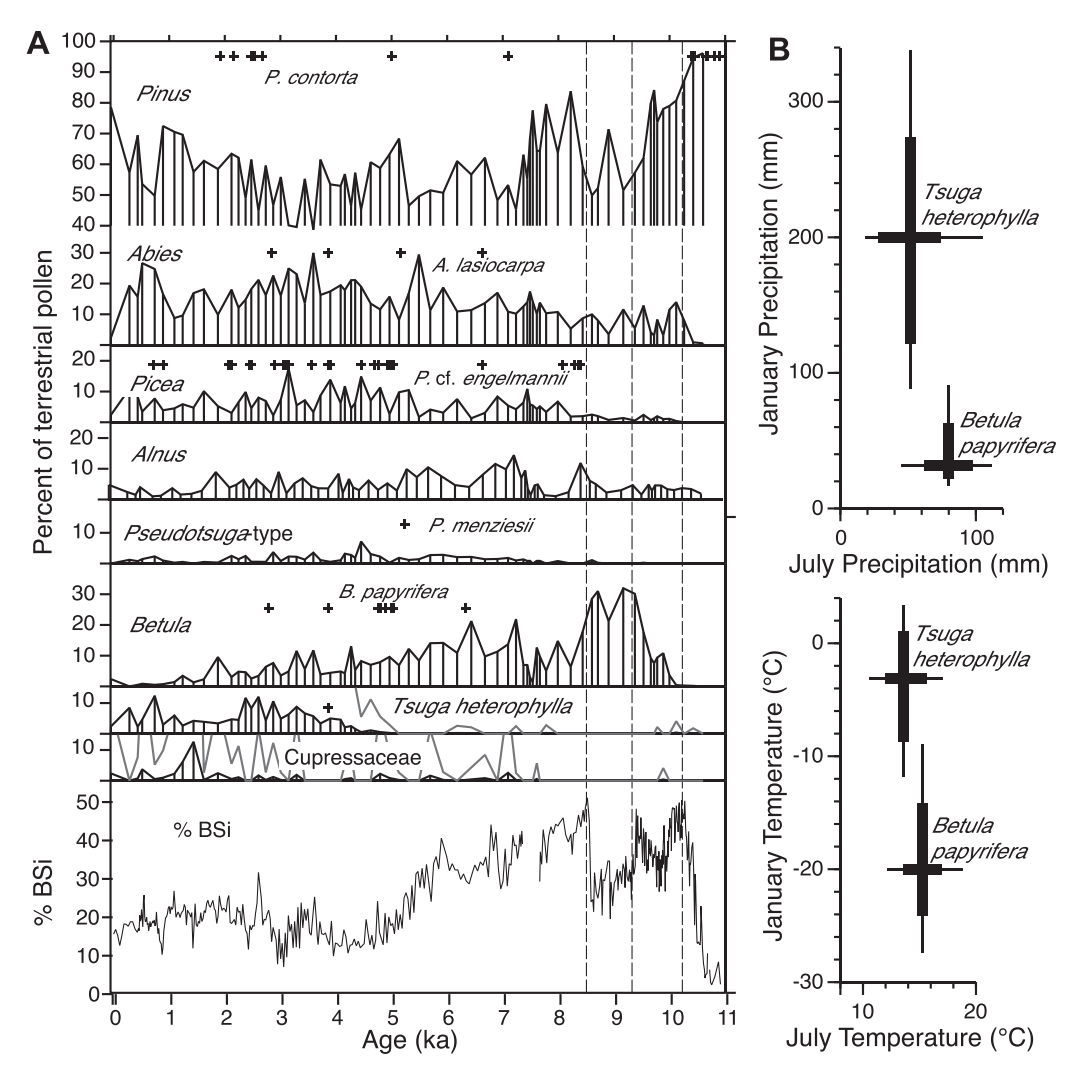


**Fig. 4.** (A) The pollen record from Eleanor Lake of the eight most common pollen types. Macrofossils (leaves and seeds) are shown by '+' symbols. Note that *Pinus* and *Abies* are plotted on the same axis. Gray lines for *Tsuga* and Cupressaceae indicate 10× exaggeration. (B) The climatic space occupied by *Tsuga heterophylla* and *Betula papyrifera*. Thin and thick lines indicate the central 80% and 50% of the distribution of climate values in the current ranges of these species (Thompson et al., 1999).

1999) and requires high phosphorous (P) concentrations suggesting these periods were marked by especially strong mixing (Bradbury, 1988; Kilham et al., 1996). In contrast, F. crotonensis and A. formosa also are typical of the spring mixing period (Reynolds, 1983; Bradbury, 1988; Kilham et al., 1996) but F. crotonensis has also been reported during summer thermal stratification and can tolerate lower nitrogen (N) and P concentrations than S. minutulus (Kilham et al., 1996; Interlandi et al., 1999; Saros et al., 2005). Further shifts in the planktonic diatom assemblage after 8.5 ka indicates further increases in thermal stratification. The Cyclotella spp., and especially C. bodanica aff. lemanica, are characteristic of lower P and N concentrations and dominate during late season stratification. This suggests warm waters and probably low precipitation and cloudiness persisting until ca 5.5 ka (Kilham et al., 1996; Interlandi et al., 1999). Periods of low BSi during the early Holocene, including the pioneer diatom assemblage, are marked by increased relative abundance of small benthic taxa belonging to the genera Staurosira and Staurosirella. These taxa tend to dominate in cold, nutrient-poor lakes where the growing season is short and/or light is limiting (Laing and Smol, 2000; Lotter and Bigler, 2000; Schmidt et al., 2004).

In the middle Holocene the transition to dominance by *F. capucina aff. gracilis* occurs during a decrease in BSi. This tychoplanktonic species is associated with near-shore areas where the

ice first melts and weak stratification in the summer, which would occur under a cooler climate with longer ice cover and generally lower productivity (Smol and Cumming, 2000; Schmidt et al., 2004), and with wetter conditions that would increase groundwater delivery of Si to the lake (Voigt et al., 2008). *F. capucina* transitions to benthic taxa during the last millennium. Taken together these shifts in the diatom assemblage suggest the importance of the controls of ice-out dates, period of mixing, and the date of the onset of thermal stratification.

The pollen record also supports a climatic interpretation of the BSi record. Major changes in BSi are paralleled by changes in *Betula* (likely produced by the tree *B. papyrifera*) and *T. heterophylla* pollen. These two tree species overlap little in geographic and climatic space: *B. papyrifera* is a deciduous tree common in continental and boreal forests with a continental climate featuring warm moist summers, whereas *T. heterophylla* is a dominant species of cool wet maritime climates (Thompson et al., 1999; Fig. 4). The period of relatively low BSi from 9.3 to 8.5 ka coincides with a decrease in *Pinus* and high levels of *Betula* pollen. This is consistent with a period of increased summer moisture, though temperatures must have remained sufficiently high to maintain diatoms indicative of thermal stratification. At 8.5 ka, the rapid increase in BSi is paralleled by a decrease in *Betula* and increase in *Pinus*, which is

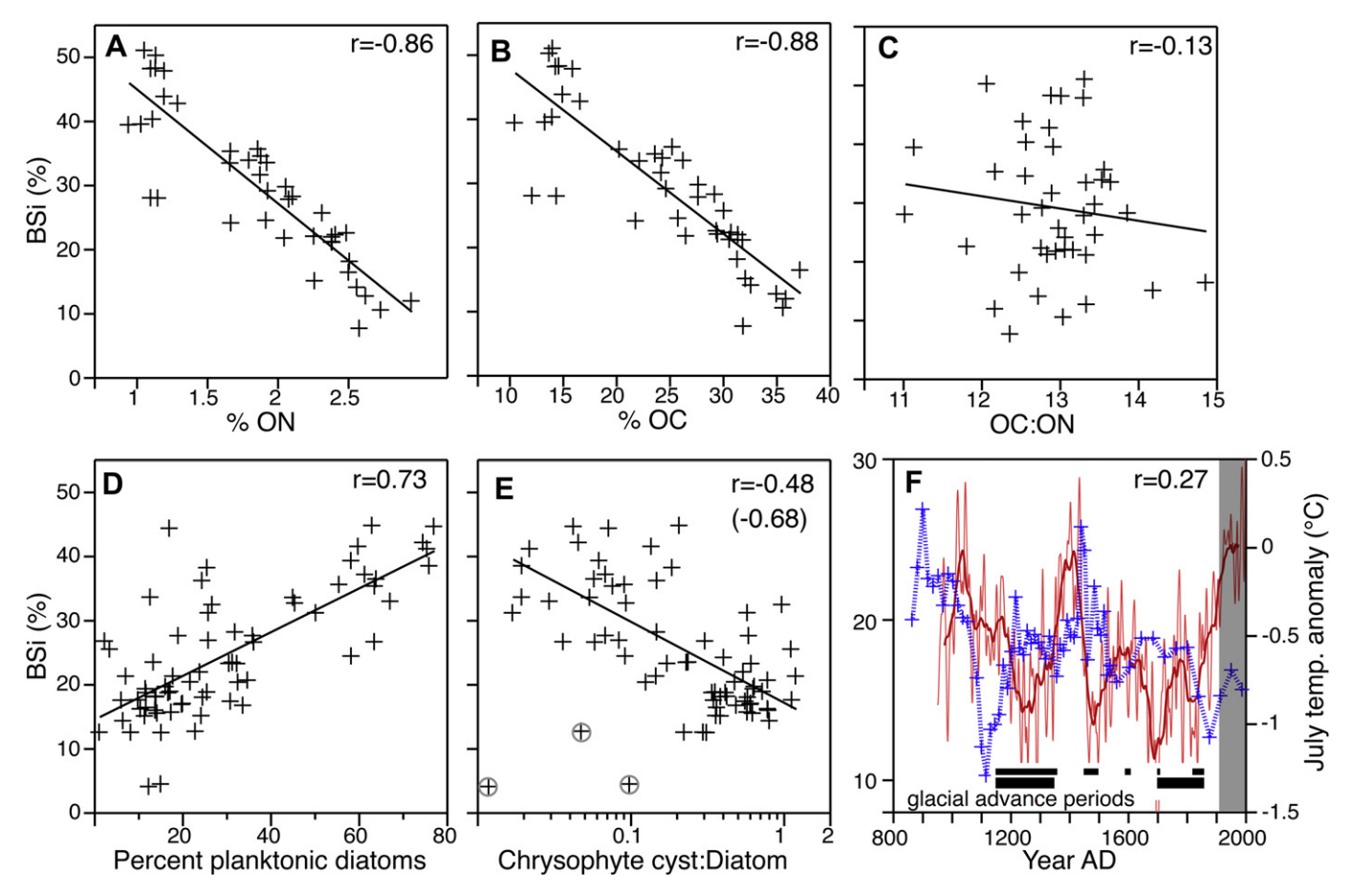


Fig. 5. Correlation of % BSi and A) organic nitrogen, B) % organic carbon, C) the ratio of organic carbon to nitrogen, D) the percentages of planktonic diatoms, and E) the ratio of chrysophyte cysts to diatoms. In panel E, removal of three outlier samples (circled) results in the stronger correlation shown in parentheses. F) % BSi over the past 1200 years plotted against mean July temperature reconstruction from the Canadian Rocky Mountains (Luckman and Wilson, 2005). Data from Luckman and Wilson (2005) were smoothed with a 20-year lowpass filter (thin line) and further smoothed by a 49-year moving average (thick line). Glacial advance periods are depicted as horizontal bars and summarized from Edwards et al. (2008), Luckman (1993) and Luckman and Wilson (2005), upper, and Menounos et al. (2009), lower. Data from Luckman and Wilson were obtained from the World Data Center for Paleoclimatology (www.ncdc.noaa.gov/paleo/paleo.html).

consistent with an onset of warm and dry conditions that would favor *Pinus* over *Betula* as an early seral species after fires (Simard, 1996). Later, over the middle to late Holocene, the progressive loss of *Betula* and increase in *Tsuga* suggests decreasing continentality and increasing winter moisture, which would result in later ice-off dates and reduced planktonic diatom blooms. Based on the sum of the above evidence, a common feature of the potential climatic controls on BSi is a combination of early-season temperature and ice-out timing effects on planktonic diatom productivity.

#### 5.2. Regional comparisons

The paleoclimate record from Eleanor Lake is in strong agreement with existing paleoclimate records from western Canada. Over the past millennium, a dendroclimatic reconstruction of maximum summer temperatures (Luckman and Wilson, 2005) compares well with % BSi (Fig. 5F), although there are discrepancies that occur within the error of the chronology (ca 100 years) in this interval and during the last century of land-use impacts on the sediment record. Over the entire Holocene, BSi follows the overall trend in summer insolation (Fig. 6). Furthermore, summer temperature inferred by compositing chironomid-based reconstructions from four sites 400 km to the south (Palmer et al., 2002; Rosenberg et al., 2004; Chase et al., 2008) follows both the millennial-scale trends and many of the early-Holocene abrupt changes in BSi (Fig. 6).

A synthesis of glacial advances from the Canadian Rocky Mountains (Menounos et al., 2009) reveal periods when climate was sufficiently cool and moist to sustain alpine glacier growth (Figs. 5F, 6). Late-Holocene glacial advances are much better documented than those during the early Holocene. At 4.3 ka, a minimum in BSi and the increase of wet-adapted *T. heterophylla* co-occurs with a regional glacial advance and some of the lowest chironomid-inferred temperatures of the Holocene (Figs. 4 and 6). Minima of BSi during the late Holocene at 2.4, 1.4, and 0.8 ka occur close in time to regional glacial advances, the most recent being coeval with the most significant neoglacial (Little Ice Age) advance (Luckman, 1993).

The sediments of neighboring Mud Lake (Fig. 1C) have been studied to reconstruct glacial activity in its watershed (Hodder et al., 2006, 2007). The Mud Lake record shows several features in agreement with Eleanor Lake. Hodder et al. (2007) found a strong negative correlation between varve thickness and spring temperature, though the mechanism behind this correlation is not clear. The overall low sedimentation at Mud Lake during the early Holocene (0.3 mm/yr) compared to the late Holocene (2.1 mm/yr) is consistent with the broad trends in BSi at Eleanor Lake. The slow sedimentation rate at Mud Lake, however, precludes detecting the early-Holocene abrupt changes observed at Eleanor Lake. Organic matter (LOI) in the Mud Lake sediment core also may reflect glaciofluvial erosional rates. The overall trend in LOI matches Eleanor Lake BSi, and during the late Holocene pulses of low LOI, likely

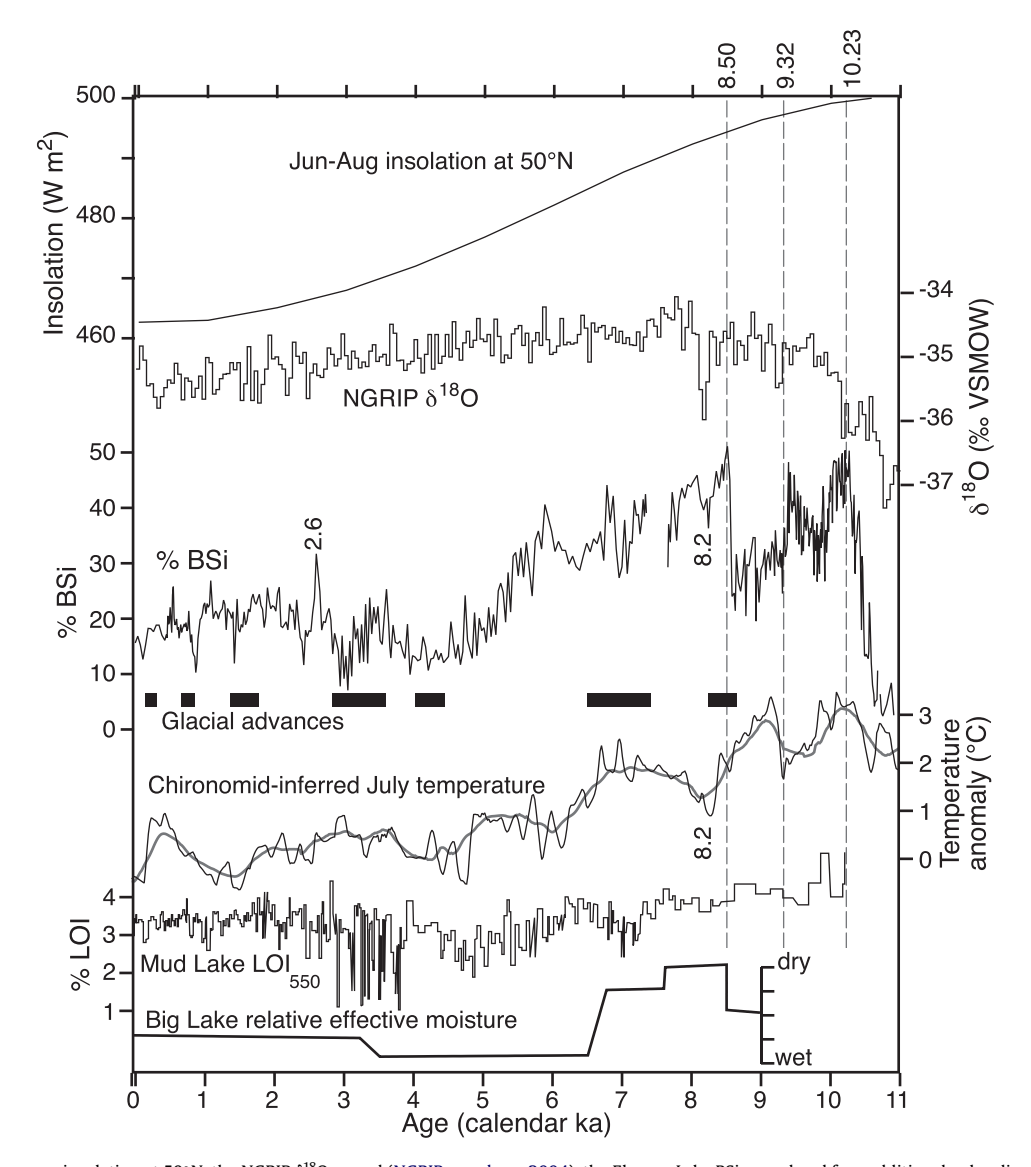


Fig. 6. Comparison of summer insolation at  $50^{\circ}$ N, the NGRIP  $\delta^{18}$ O record (NGRIP members, 2004), the Eleanor Lake BSi record and four additional paleoclimate records from British Columbia. Vertical dashed lines indicate abrupt changes in the BSi time series; other events on the BSi record at 2.6 ka and 8.2 ka also are highlighted. Glacial-advance periods are from Menounos et al. (2009). The composite record of July temperature anomalies based on chironomid assemblages from four sites with well-constrained chronologies (Fig. 1): Frozen Lake (Rosenberg et al., 2004), North Crater Lake and Lake-of-the-Woods (Palmer et al., 2002), and Windy Lake (Chase et al., 2008). Thin and thick lines are loess-smoothed temperature anomalies (based on a 0–2 ka base period) in 300-yr and 750-yr windows, respectively (Cleveland, 1979). Mud Lake LOI is from Hodder et al. (2006). Relative effective moisture at Big Lake was inferred from multiple proxies, including diatom assemblages and pollen (Bennett et al., 2001).

resulting from glacier advances upstream of Mud Lake, occur close in time to minima in BSi at Eleanor Lake (Fig. 6).

Last, multi-proxy records of relative moisture from Big Lake located 156 km to the southwest (Bennett et al., 2001) and from Felker Lake located 186 km to the west (Galloway et al., 2011) are in good agreement with our BSi record. These records show a warming and drying at ca 8.5 ka, in agreement with increases in BSi and in subsequent increases in *C. bodanica* aff. *lemanica* (indicating stratification). During the middle Holocene, however, Big Lake shows the onset of cool/wet conditions several millennia earlier than suggested by BSi and pollen at Eleanor Lake, and Felker Lake shows great variability in diatom-inferred salinity.

In summary, the chironomid records, the glacial advance records, the sedimentation study at Mud Lake, and the nearby multi-proxy paleolimnological records support the general trends and many specific features found at Eleanor Lake. Our BSi record is unmatched at other sites in its temporal resolution, yet there is no

evidence that clearly contradicts specific aspects of the BSi record. Thus, the striking abrupt and persistent changes in BSi during the early Holocene deserve special attention.

#### 5.3. Correlation with proxies of solar activity

Variation in our BSi record is similar to that in cosmogenic nuclide indices of solar irradiance. In particular, between 11 and 8 ka detrended BSi is strongly correlated with  $^{10}\text{Be}$  flux ( $r\!=\!0.70$ ;  $P\!<\!0.001$ ) and the production rate of  $^{14}\text{C}$  ( $r\!=\!0.55$ ;  $P\!<\!0.001$ ) (Fig. 7). Introducing lags does not further increase the correlations between these independently dated series. Because the production rates of cosmogenic nuclides increase with decreased solar irradiance when solar winds are weak and the geomagnetic field is strong, these correlations are opposite in sign to that expected from direct solar forcing. After the gap in the BSi record at 7.2–7.5 ka, BSi remains correlated with the production rate of  $^{14}\text{C}$  (maximum

correlation = 0.24 with a 50-year lag; P = 0.02), but not with  $^{10}$ Be flux (r = -0.03; P > 0.5). Steinhilber et al. (2009) recently computed a 9300 record of total solar irradiance (TSI) using the  $^{10}$ Be flux record to reconstruct the interplanetary magnetic field, which is strongly correlated with TSI. We found that the TSI record of Steinhilber et al. (2009), after detrending and smoothing, is strongly correlated (r = -0.68) with the  $^{10}$ Be flux record of Marchitto et al. (2010) used in this study. This is not surprising considering that TSI was computed from a portion of the raw  $^{10}$ Be flux data used in Marchitto et al. (2010), who composited the  $^{10}$ Be records from the GISP2 and GRIP cores spanning the entire Holocene. For the period 0–9.3 ka, BSi is weakly correlated with TSI (r = -0.16), as expected based on the low BSi $^{-10}$ Be flux correlation over this period. Therefore, use of the TSI record does not affect our conclusions with the exception that it is limited to the period after 9.3 ka.

#### 6. Discussion

#### 6.1. Abrupt climate shifts

Several abrupt climate changes have been detected during the early Holocene throughout the northern hemisphere and have been related to the dynamics of the Laurentide Ice Sheet (Alley et al., 2003). The BSi record from Eleanor Lake also displays many early Holocene abrupt changes, which are supported by diatom and pollen data from the same core. For many of these events, however, the direction of the climate change, the timing of the events, and the persistence following the abrupt change differ from the abrupt changes reconstructed elsewhere in the northern hemisphere. Here we discuss these abrupt changes with respect to evidence elsewhere and potential linkages to large-scale climatic forcings.

The abrupt BSi increase at 8.5 ka, which occurred within 2-cm of sediment (ca 30 years), is dated directly by an AMS  $^{14}$ C age of leaf material ( $2\sigma$  calibrated age range = 8.43–8.60 ka). This places it coeval with the proposed age of a catastrophic ice sheet collapse and drainage of glacial lakes Agassiz and Ojibway (peaking at ca 8.47 ka with smaller events through 8.35 ka; Hillaire-Marcel et al., 2007). This finding contributes to growing evidence from the North Atlantic region that cold events were initiated ca 200 yr prior to the 8.2 ka event detected in the Greenland ice cores, and that there may be multiple climatic perturbations between 8.5 and 8 ka (Hu et al., 1999; Axford et al., 2009; Daley et al., 2009). The 8.5 ka event at Eleanor Lake is distinct from the North Atlantic records, however, in that the abrupt shift was not a decadal or centennial-scale excursion, but rather a change to a new state that persisted for millennia.

The mechanism driving an abrupt and persistent climate change at 8.5 ka is not clear. One potential cause could be a rapid reorganization of the meridional structure of atmospheric circulation as a response to the early Holocene ice-sheet collapse. Similar explanations have been proposed for lower-resolution records that show similar early-Holocene climatic fluctuations but are located in Alberta closer to the 8.5 ka ice sheet (MacDonald and Case, 2000). A larger synthesis of paleoclimate records shows that the climatic response to the ca 8.2 ka event was more step-like west of the Great Lakes region, compared to the "pulsed" response in the north Atlantic region (Shuman et al., 2002). Climatic simulations indicate that with ice-sheet loss, there was an increased onshore flow due to a substantially reduced glacial anticyclone and an eastward shift of the polar jet (Kutzbach et al., 1993; Pollard et al., 1998). This interpretation is supported by a data synthesis of the timing of the Holocene thermal maximum in the region north of Eleanor Lake (CAPE, 2001).

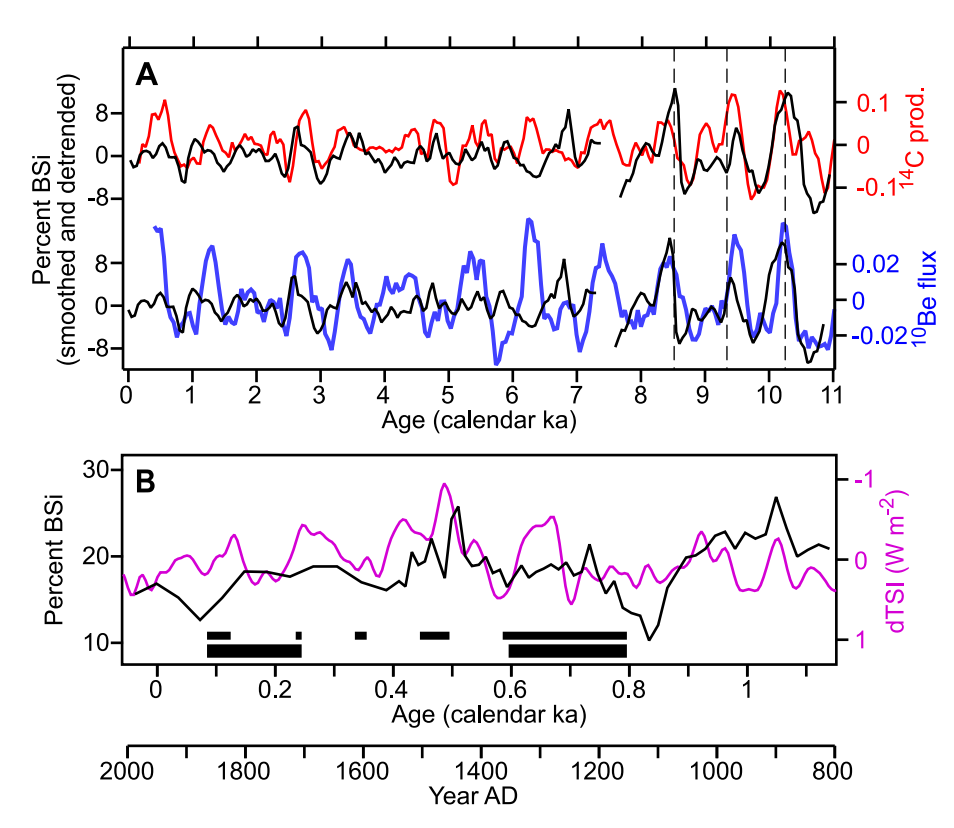


Fig. 7. A) The Eleanor Lake biogenic silica (BSi) record compared to proxies of solar activity. BSi is plotted with <sup>14</sup>C production rate (top) and <sup>10</sup>Be flux (bottom). Solar proxies and BSi data are smoothed (ca 100 year running mean) and detrended (high-pass filter at 1/1800 year<sup>-1</sup>) similarly following Marchitto et al. (2010). Dashed lines are abrupt changes in the BSi record. B) The last 1200 years of the raw BSi record and the total solar irradiance record (dTSI) of Steinhilber et al. (2009). Note the reversed axis of dTSI. Horizontal black bars are glacial advance periods as in Fig. 5.

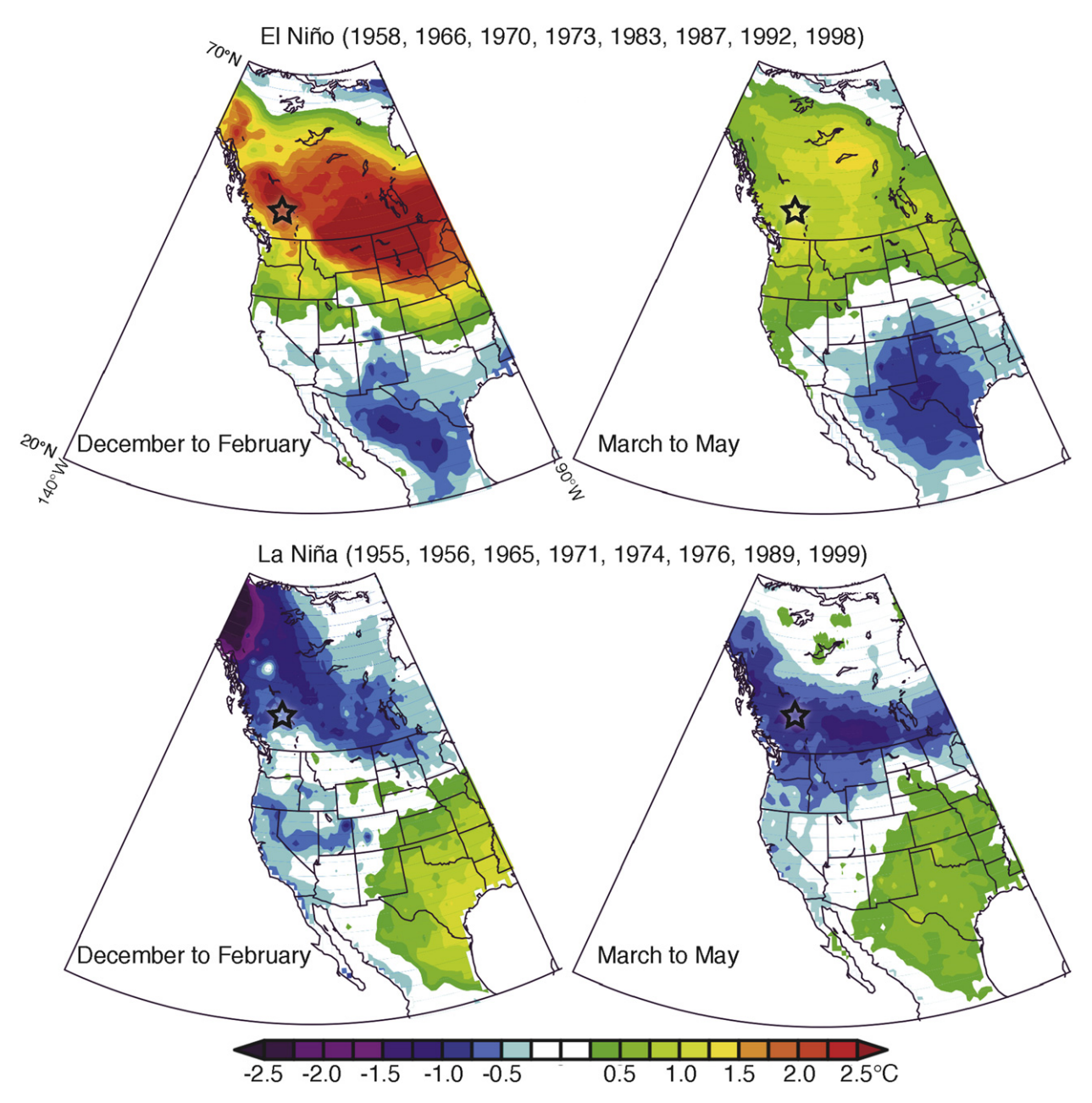


Fig. 8. Surface air temperature composite anomalies for El Niño winter and spring conditions (top) and La Niña winter and spring conditions (bottom). Each anomaly map is the three-month mean compared to a climatology for 1950–1999. The location of Eleanor Lake is shown by a star. Gridded temperature data are from the University of Delaware (Legates and Willmott, 1990); data access and graphics were provided by the NOAA/OAR/ESRL PSD, Boulder, Colorado, USA, from their Web site at http://www.esrl.noaa.gov/psd/.

At the time of the North Atlantic 8.2 ka event, the BSi record from Eleanor Lake shows a brief decadal-scale cooling embedded within a century-scale cooling, a pattern similar to that in the NGRIP isotope record and thought to be restricted to the North Atlantic (Rohling and Pälike, 2005). An 8.2 ka event is evident in several chironomid records in western Canada (Fig. 6; Chase et al., 2008; Bunbury and Gajewski, 2009) and in a glacial-advance period of 8.59–8.18 ka, of which the majority of evidence falls closer to 8.2 ka than to 8.5 ka (Menounos et al., 2009). At Eleanor Lake, the 8.2 ka event is distinct from the abrupt and persistent change at 8.5 ka, implying that the mechanisms driving this event are likely distinct from those that produced the 8.5 ka event.

The abrupt BSi decrease at 9.3 ka presents a case similar to the 8.5 ka event. Our  $^{14}$ C dating of a leaf macrofossil of this event ( $2\sigma$  calibrated age range = 9.30–9.47 ka) occurs during the same period

as a recently proposed outburst flood from Lake Superior that may have triggered the 9.3 ka cold period detected in the Greenland ice cores (Yu et al., 2010). This event also has been identified in various locations around the North Atlantic (Marshall et al., 2007; Fleitmann et al., 2008; Axford et al., 2009). As with the 8.5 ka event, the 9.3 ka event at Eleanor Lake was a persistent change rather than a century-scale excursion. A coeval abrupt change in chironomid-inferred temperatures occurred at other sites in the same region (Fig. 6). However, the conflicting interpretation of the direction of climate change at 9.3 ka inferred from the chironomids (warming) and BSi (cooling) deserves further investigation and may be explained by differences in the seasonal sensitivities of each proxy (i.e., later summer season for chironomids than BSi), or by changes in precipitation that may affect the BSi/temperature relationship. Regardless of the seasonal expression of climate change,

the abrupt and persistent character of the 9.3 ka event suggests a similar mechanism to that responsible at 8.5 ka.

The initial, rapid, increase of BSi from 10.8 to 10.2 ka likely reflects both continued warming and establishing biogeochemical cycles at Eleanor Lake. This co-occurs with a transition from benthic to planktonic diatoms, probably resulting from increased nutrient availability and earlier ice-out. The regional chironomid temperature reconstruction and the GRIP ice core also indicate continued warming during this period (Fig. 6). This increase in BSi is terminated by an abrupt reversal beginning at 10.23 ka. Björck et al. (2001) reported a hemispheric-wide brief cooling event at 10.3 ka, though this event is not manifest as a brief cooling at Eleanor Lake but rather as a peak and reversal in the trend of BSi.

#### 6.2. Antiphased response to solar forcing?

Solar-irradiance explanations of climate changes in the early Holocene have been proposed by multiple studies, including at times of specific events in the Eleanor Lake record (Björck et al., 2001; Hu et al., 2003; Marshall et al., 2007; Plunkett and Swindles, 2008). In contrast with these previous studies, our study shows a strong negative correlation of regional climate with solar irradiance during the early Holocene, and possibly extending into the middle and late Holocene (Fig. 7). In addition, detrended BSi before 8 ka is correlated with proxies from other regions where possible solar-climate linkages have been reported, including the ice-rafted debris record in the North Atlantic (r = 0.50: P = 0.01: Bond et al., 2001), and the BSi record from Arolik Lake in southwest Alaska (r = -0.46; P = 0.02; Hu et al., 2003). Such a negative correlation is consistent with the expectation that subtle variability of solar irradiance on Holocene time scales requires an internal feedback mechanism within the climate system to produce regional climate changes (Shindell et al., 2001).

One possible mechanism driving a solar irradiance connection to climate may lie in the El Niño oscillation operating as a dynamical response to solar fluctuations, with La Niña-like conditions predominating during low solar activity and El Niño-like conditions predominating during high solar activity (Mann et al., 2005). Recently, Marchitto et al. (2010) have shown that sea-surface temperatures, as measured by Mg/Ca ratios of a planktonic foraminifer in a sediment core from Soledad Basin in the eastern tropical Pacific Ocean, are significantly related to the <sup>10</sup>Be and <sup>14</sup>C solar proxies, with warm (El Niño-like) temperatures predominating during low solar activity. The detrended Eleanor Lake BSi record, in turn, is positively correlated with the early Holocene sea surface temperatures at Soledad Basin (r = 0.41; P = 0.04). El Niño variability is clearly expressed at the study site, despite its northerly location in central British Columbia. Composite anomaly maps of surface air temperature for the eight largest El Niño events since 1950 show winter temperatures in east-central British Columbia 2.5 °C warmer than average, and spring temperatures 1.5 °C warmer than average (Legates and Willmott, 1990; Fig. 8). Likewise, for the eight years with strong La Niña conditions, both winter and spring conditions are 1 °C colder than average. Therefore, centennial-scale trends in El Niño-like conditions, driven by solar activity variations, may explain the anti-phased relationship between solar activity and temperature at our study site. Weaker variations in solar activity in the middle to late Holocene may have been insufficient to maintain these patterns (Marchitto et al., 2010).

Another mechanism driving a solar irradiance connection to climate may lie in the interaction of solar irradiance and atmospheric circulation as influenced by the Laurentide ice sheet. In the presence of an ice sheet, decreased irradiance would have enhanced the ocean-land temperature contrast and strengthened the glacial anticyclonic circulation, pulling warm air northward to the west of the ice

sheet and cold air southward to the east. Conversely, with higher irradiance and a weaker anticyclone, moist Pacific air penetrated further east, such as during the *Betula* period between 9.3 and 8.5 ka.

Two model simulations of the interaction of atmospheric circulation and the Laurentide Ice Sheet provide support for this scenario. First, the GENESIS v.2 GCM showed a region of climatic warming west of the remnant Laurentide Ice Sheet at 10 ka that is attributable to the glacial anticyclone (Pollard et al., 1998; CAPE, 2001). Second, a simple model of the effect of an ice sheet on the atmospheric stationary wave suggests the effect of a large ice sheet has hemispheric-scale impact on the location of the polar jet stream (Roe and Lindzen, 2001). The steep gradient created by the polar jet, which may shift position due to strength of the glacial anticyclone downstream, may have large climatic effects at our site. A similar effect of the position of the jet causing abrupt changes in the winter and early-season climate in the eastern United States was proposed by Kirby et al. (2002). After 8.5 ka, the ice sheet was significantly reduced in extent and elevation, such that the glacial anticyclone may not have directly affected the Eleanor Lake area, 1200 km to the west (Fig. 1).

Following the collapse of the Laurentide Ice Sheet, solar-climate linkages are weak. A continued negative solar-climate correlation is most evident during two periods. First, large fluctuations in BSi at 3 ka parallel the <sup>14</sup>C production rate. A BSi peak at 2.6 ka may be related to climatic cooling at ca 2.7 ka documented elsewhere and attributed to the irradiance minima at this time (Fig. 7A; Plunkett and Swindles, 2008). Second, BSi reaches a local minimum during moderate solar activity at ca 0.8 ka (Fig. 7B; Steinhilber et al., 2009), the time immediately preceding a regional glacial advance in the Canadian Rocky Mountains (Luckman, 1993). However, other studies from the Canadian Rocky Mountains report that solar minima are correlated with glacial advances (Luckman and Wilson, 2005; Koch et al., 2007) and high lake levels (Hallett et al., 2003) over the past millennium. More high-resolution paleoclimate records spanning the past 1500 years are needed to explore potential linkages with solar variability in this region.

#### 6.3. Conclusions

The multi-proxy climate record from Eleanor Lake reveals a complex Holocene history with an early Holocene marked by abrupt and persistent climate changes and a late Holocene marked by punctuated cool periods. The two largest such abrupt shifts occurred at 8.5 ka and 9.3 ka, coeval with Lake Agassiz outburst floods and rapid reduction of ice sheet and proglacial lake extent downstream of the study site. These events constitute major boundary-condition shifts that may have propagated upstream through shifting meridional structure of atmospheric circulation. A potential link of solar activity with El-Niño-like patterns may explain additional abrupt shifts, especially during the relatively large solar activity fluctuations during the early Holocene. Another mechanism may lie in the changing strength of the glacial anticyclone and its effects on the location of the polar jet. These mechanisms also explain the antiphase correlatation between climate and solar forcing and why correlations are strongest before 8 ka. Overall our high-resolution sediment record from Eleanor Lake reveals intriguing new features of Holocene climate change in western Canada. Additional paleoclimate reconstructions and model simulations are needed to verify these findings and to evaluate the mechanistic explanations discussed here.

#### Acknowledgements

Funding was provided by the National Science Foundation award DEB-0212917 (FSH, DGG, SCF) and the Packard Foundation

(FSH). Laboratory work was assisted by Lauren Roschen (biogenic silica, CHN, loss-on-ignition, and pollen processing), Jian Tian (X-ray diffraction measurements), and Paul Henne (<sup>210</sup>Pb measurements). We thank Tom Brown for handling the AMS radiocarbon dates. We greatly appreciate comments from P.J. Bartlein and two anonymous reviewers.

#### References

- Alley, R.B., Marotzke, J., Nordhaus, W.D., Overpeck, J.T., Peteet, D.M., Pielke, R.A., Pierrehumbert, R.T., Rhines, P.B., Stocker, T.F., Talley, L.D., Wallace, J.M., 2003. Abrupt climate change. Science 299, 2005—2010.
- Axford, Y., Briner, J.R., Miller, G.H., Francis, D.R., 2009. Paleoecological evidence for abrupt cold reversals during peak Holocene warmth on Baffin Island, Arctic Canada. Quat. Res. 71, 142–149.
- Battarbee, R.W., 2000. Palaeolimnological approaches to climate change, with special regard to the biological record. Quat. Sci. Rev. 19, 107–124.
- Battarbee, R.W., Jones, V.J., Flower, R.J., Cameron, N.G., Bennion, H., Carvalho, L., Juggins, S., 2001. Diatoms. In: Smol, J.P., Birks, H.J.B., Last, W.M. (Eds.), Tracking Environmental Change Using Lake Sediments. DPER, vol. 3. Kluwer Academic Publishers, Dordrecht, pp. 155–202.
- Bennett, J.R., Cumming, B.F., Leavitt, P.R., Chiu, M., Smol, J.P., Szeicz, J., 2001. Diatom, pollen, and chemical evidence of postglacial climatic change at Big Lake, south-central British Columbia, Canada. Quat. Res. 55, 332–343.
- Björck, S., Muscheler, R., Kromer, B., Andresen, C.S., Heinemeier, J., Johnsen, J., Johnsen, S.J., Conley, D., Koc, N., Spurk, M., Veski, S., 2001. High-resolution analyses of an early Holocene climate event may imply decreased solar forcing as an important climate trigger. Geology 29, 1107—1110.
- Bond, G., Kromer, B., Beer, J., Muscheler, R., Evans, M.N., Showers, W., Hoffmann, S., Lotti-Bond, R., Hajdas, I., Bonani, G., 2001. Persistent solar influence on north Atlantic climate during the Holocene. Science 294, 2130–2136.
- Bradbury, J.P., 1988. A climatic—limnologic model of diatom succession for paleolimnological interpretation of varved sediments at Elk Lake, Minnesota. J. Paleolimnol. 1, 115–131.
- Bunbury, J., Gajewski, K., 2009. Postglacial climates inferred from a lake at treeline, southwest Yukon Territory, Canada. Quat. Sci. Rev. 28, 354–369.
- CAPE Members, 2001. Holocene paleoclimate data from the Arctic: testing models of global climate change. Quat. Sci. Rev. 20, 1275–1287.
- Chase, M., Bleskie, C., Walker, I.R., Gavin, D.G., Hu, F.S., 2008. Midge-inferred Holocene summer temperatures in Southeastern British Columbia, Canada. Palaeogeogr. Palaeoclimatol. Palaeoecol. 257, 244–259.
- Clague, J.J., Evans, S.G., Rampton, V.N., Woodsworth, G.J., 1995. Improved age estimates for the White River and Bridge River tephras. Can. J. Earth Sci. 32, 1172–1179.
- Cleveland, W.S., 1979. Robust locally weighted regression and smoothing scatterplots. J. Am. Stat. Assoc. 74, 829–836.
- Cumming, B.F., Wilson, S.E., Hall, R.I., Smol, J.P., 1995. Diatoms from British Columbia (Canada) Lakes and their relationship to salinity, nutrients and other limnological variables. Biblioth. Diatomol. 31, 207.
- Daley, T.J., Street-Perrott, F.A., Loader, N.J., Barber, K.E., Hughes, P.D.M., Fisher, E.H., Marshall, J.D., 2009. Terrestrial climate signal of the "8200 yr BP cold event" in the Labrador Sea region. Geology 37, 831–834.
- Denton, G.H., Anderson, R.F., Toggweiler, J.R., Edwards, R.L., Schaefer, J.M., Putnam, A.E., 2010. The Last Glacial termination. Science 328, 1652–1656.
- Dyke, A.S., Moore, A., Robertson, L., 2003. Deglaciation of North America. Geological Survey of Canada Open File 1574.
- Edwards, T.W.D., Birks, S.J., Luckman, B.H., MacDonald, G.M., 2008. Climatic and hydrologic variability during the past millennium in the eastern Rocky Mountains and northern Great Plains of western Canada. Ouat. Res. 70, 188–197.
- Faegri, K., Iversen, J., 1992. Textbook of Pollen Analysis. Hafner, New York. Fleitmann, D., Mudelsee, M., Burns, S.J., Bradley, R.S., Kramers, J., Matter, A., 2008.
- Fleitmann, D., Mudelsee, M., Burns, S.J., Bradley, R.S., Kramers, J., Matter, A., 2008. Evidence for a widespread climatic anomaly at around 9.2 ka before present. Paleoceanography 23, PA1102.
- Foit, F.F., Gavin, D.G., Hu, F.S., 2004. The tephra stratigraphy of two lakes in south-central British Columbia, Canada and its implications for mid-late Holocene volcanic activity at Glacier Peak and Mount St. Helens, Washington, USA. Can. J. Earth Sci. 41, 1401–1410.
- Galloway, J.M., Lenny, A.M., Cumming, B.F., 2011. Hydrological change in the central interior of British Columbia, Canada: diatom and pollen evidence of millennial-to-centennial scale change over the Holocene. Journal of Paleolimnology. doi:10.1007/s10933-010-9490-9.
- Hallett, D.J., Mathewes, R.W., Walker, R.C., 2003. A 1000-year record of forest fire, drought and lake level change in southeastern British Columbia. Holocene 13, 751–761.
- Hillaire-Marcel, C., de Vernal, A., Piper, D.J.W., 2007. Lake Agassiz final drainage event in the northwest North Atlantic. Geophys. Res. Lett. 34, L15601.
- Hilton, J., 1985. A conceptual framework for predicting the occurrence of sediment focusing and sediment redistribution in small lakes. Limnol. Oceanogr. 30, 1141–1143.
- Hodder, K.R., Desloges, J.R., Gilbert, R., 2006. Pattern and timing of sediment infill at glacier-fed Mud Lake: implications for lateglacial and Holocene environments in the Monashee Mountain region of British Columbia, Canada. Holocene 16, 705–716.
- Hodder, K.R., Gilbert, R., Desloges, J.R., 2007. Glaciolacustrine varved sediment as an alpine hydroclimatic proxy. J. Paleolimnol. 38, 365—394.

- Hu, F.S., Slawinski, D., Whight Jr., H.E., Ito, E., Johnson, R.G., Kelts, K.R., McEwan, R.F., Boedigheimer, A., 1999. Abrupt changes in North American climate during the early Holocene. Nature 400, 437–440.
- Hu, F.S., Kaufman, D., Yoneji, S., Nelson, D., Shemesh, A., Huang, Y., Tian, J., Bond, G., Clegg, B., Brown, T., 2003. Cyclic variation and solar forcing of Holocene climate in the Alaskan subarctic. Science 301, 1890—1893.
- Interlandi, S.J., Kilham, S.S., Theriot, E.C., 1999. Responses of phytoplankton to varied resource availability in large lakes of the Greater Yellowstone Ecosystem. Limnol. Oceanogr. 44, 668–682.
- Kilham, S.S., Theriot, E.C., Fritz, S.C., 1996. Linking planktonic diatoms and climate change in the large lakes of the Yellowstone ecosystem using resource theory. Limnol. Oceanogr. 41, 1052–1062.
- Kirby, M.E., Mullins, H.T., Patterson, W.P., Burnett, A.W., 2002. Late glacial-Holocene atmospheric circulation and precipitation in the northeast United States inferred from modern calibrated stable oxygen and carbon isotopes. Geol. Soc. Am. Bull. 114, 1326—1340.
- Kleiven, H.F., Kissel, C., Laj, C., Ninnemann, U.S., Richter, T.O., Cortijo, E., 2008. Reduced North Atlantic Deep Water coeval with the glacial Lake Agassiz freshwater outburst. Science 319, 60–64.
- Koch, J., Osborn, G.D., Clague, J.J., 2007. Pre-'Little Ice Age' glacier fluctuations in Garibaldi Provincial Park, Coast Mountains, British Columbia, Canada. Holocene 17. 1069—1078.
- Krammer, K., Lange-Bertalot, H., 1991. Bacillariophyceae. In: Ettl, H., Gerloff, J., Heynig, H., Mollenhauser, D. (Eds.), Süßwasserflora von Mitteleuropa, 2 1—4 Gustav Fisher Verlag, Stuttgrat/Jena.
- Gustav Fisher Verlag, Stuttgrat/Jena.
  Kutzbach, J.E., Guetter, P.J., Behling, P.J., Selin, R., 1993. Simulated climatic changes: results of the COHMAP climate-model experiments. In: Wright, H.E. (Ed.), Global Climates Since the Last Glacial Maximum. University of Minnesota Press, Minneapolis, pp. 24–93.
- Laing, T.E., Smol, J.P., 2000. Factors influencing diatom distributions in circumpolar treeline lakes of northern Russia. J. Phycol. 36, 1035–1048.
- Legates, D.R., Willmott, C.J., 1990. Mean seasonal and spatial variability in global surface air temperature. Theor. Appl. Climatol. 41, 11–21.
- Lotter, A.F., Bigler, C., 2000. Do diatoms in the Swiss Alps reflect the length of ice-cover? Aquat. Sci. 62, 125–141.
- Lotter, A.F., Birks, H.J.B., Hofmann, W., Marchetto, A., 1997. Modern diatom, cladocera, chironomid, and chrysophyte cyst assemblages as quantitative indicators for the reconstruction of past environmental conditions in the Alps. 1. Climate J. Paleolimnol. 18, 395–420.
- Luckman, B.H., 1993. Glacial fluctuation and tree-ring records for the last millenium in the Canadian Rockies. Quat. Sci. Rev. 12, 441–450.
- Luckman, B.H., Wilson, R.J.S., 2005. Summer temperatures in the Canadian Rockies during the last millennium: a revised record. Clim. Dyn. 24, 131–144.
- MacDonald, G.M., Case, R.A., 2000. Biological evidence of multiple temporal and spatial scales of hydrological variation in the western interior of Canada. Quat. Int. 67, 133–142.
- Mann, M.E., Cane, M.A., Zebiak, S.E., Clement, A., 2005. Volcanic and solar forcing of the tropical Pacific over the past 1000 years. J. Climate 18, 447–456.
- Marchitto, T.M., Muscheler, R., Ortiz, J.D., Carriquiry, J.D., van Geen, A., 2010. Dynamical response of the tropical Pacific Ocean to solar forcing during the early Holocene. Science 330, 1378–1381.
- Marshall, J.D., Lang, B., Crowley, S.F., Weedon, G.P., van Calsteren, P., Fisher, E.H., Holme, R., Holmes, J.A., Jones, R.T., Bedford, A., Brooks, S.J., Bloemendal, J., Kiriakoulakis, K., Ball, J.D., 2007. Terrestrial impact of abrupt changes in the North Atlantic thermohaline circulation: Early Holocene, UK. Geology 35, 639–642.
- Massey, N.W.D., MacIntyre, D.G., Desjardins, P.J., Cooney, R.T., 2005. Digital Geology Map of British Columbia. B.C. Ministry of Energy and Mines, Geofile 2005–7.
- Menounos, B., Osborn, G., Clague, J.J., Luckman, B.H., 2009. Latest Pleistocene and Holocene glacier fluctuations in western Canada. Quat. Sci. Rev. 28, 2049–2074.
- Meyers, P.A., Lallier-Vergas, E., 1999. Lacustrine sedimentray organic matter records of Late Quaternary paleoclimates. J. Paleolimnol. 21, 345–372.
- Moore, D.M., Reynolds Jr., R.C., 1997. X-Ray Diffraction and the Identification and Analysis of Clay Minerals. Oxford Univ. Press, New York.
- Mortlock, R.A., Froelich, P.N., 1989. A simple method for the rapid-determination of biogenic opal in pelagic marine sediments. Deep-Sea Res. Part A-Oceanogr. Res. Pap. 36, 1415–1426.
- NGRIP (North Greenland Ice Core Project) members, 2004. High-resolution record of Northern Hemisphere climate extending into the last interglacial period. Nature 431, 147–151.
- Palmer, S., Walker, I., Heinrichs, M., Hebda, R., Scudder, G., 2002. Postglacial midge community change and Holocene palaeotemperature reconstructions near treeline, southern British Columbia (Canada). J. Paleolimnol. 28, 469–490.
- Patrick, R., Reimer, C.W., 1975, The diatoms of the United States, exclusive of Alaska and Hawaii. Academy of Natural Sciences of Philadelphia Monograph No. 13, vol. 2, Part 1, 688 p..
- Plunkett, G., Swindles, G.T., 2008. Determining the Sun's influence on Lateglacial and Holocene climates: a focus on climate response to centennial-scale solar forcing at 2800 cal. BP. Quat. Sci. Rev. 27, 175–184.
- Pollard, D., Bergengren, J.C., Stillwell-Soller, L.M., Felzer, B., Thompson, S.L., 1998. Climate simulations for 10000 and 6000 years BP using the GENESIS global climate model. Paleoclimates Data and Modelling 2, 183—218.
- Reimer, P.J., Baillie, M.G.L., Bard, E., Bayliss, A., Beck, J.W., Bertrand, C.J.H., Blackwell, P.G., Buck, C.E., Burr, G.S., Cutler, K.B., Damon, P.E., Edwards, R.L., Fairbanks, R.G., Friedrich, M., Guilderson, T.P., Hogg, A.G., Hughen, K.A., Kromer, B., McCormac, G., Manning, S., Ramsey, C.B., Reimer, R.W., Remmele, S.,

- Southon, J.R., Stuiver, M., Talamo, S., Taylor, F.W., van der Plicht, J., Weyhenmeyer, C.E., 2004. IntCal04 terrestrial radiocarbon age calibration, 0–26 cal kyr BP. Radiocarbon 46, 1029–1058.
- Reynolds, C.S., 1983. A physiological interpretation of the dynamic responses of populations of a planktonic diatom to physical variability of the environment. New Phytol. 95, 41–53.
- Roe, G.H., Lindzen, R.S., 2001. The mutual interaction between continental-scale ice sheets and atmospheric stationary waves. J. Climate 14, 1450—1465.
- Rohling, E.J., Pälike, H., 2005. Centennial-scale climate cooling with a sudden cold event around 8,200 years ago. Nature 434, 975—979.
- Rosenberg, S.A., Walker, I.R., Mathewes, R.W., Hallett, D.J., 2004. Midge-inferred Holocene climate history of two subalpine lakes in southern British Columbia, Canada. Holocene 14. 258–271.
- Saros, J.E., Michel, T.J., Interlandi, S.J., Wolfe, A.P., 2005. Resource requirements of *Asterionella formosa* and *Fragilaria crotonensis* in oligotrophic alpine lakes: implications for recent phytoplankton community reorganizations. Can. J. Fish. Aquat. Sci. 62, 1681–1689.
- Schmidt, R., Kamenik, C., Lange-Bertalot, H., Klee, R., 2004. Fragilaria and Staurosira (Bacillariophyceae) from sediment surfaces of 40 lakes in the Austrian Alps in relation to environmental variables, and their potential for palaeoclimatology. J. Paleolimnol. 63, 171–189.
- Shindell, D.T., Schmidt, G.A., Mann, M.E., Rind, D., Waple, A., 2001. Solar forcing of regional climate change during the Maunder Minimum. Science 294, 2149–2152.
- Shuman, B., Bartlein, P., Logar, N., Newby, P., Webb, T., 2002. Parallel climate and vegetation responses to the early Holocene collapse of the Laurentide Ice Sheet. Ouat. Sci. Rev. 21, 1793–1805.

- Simard, S.W., 1996. Ecological and silvicultural characteristics of paper birch in the southern interior of British Columbia. In: Comeau, P.G., Harper, G.J., Blache, M.E., Boateng, J.O., Thomas, K.D. (Eds.), Ecology and Management of British Columbia Hardwoods. Workshop Proceedings, Dec. 1–2, 1993, Richmond, B.C. British Columbia Ministry of Forestry, Victoria, BC, pp. 157–167. FRDA Rep. 255.
- Smol, J.P., Cumming, B.F., 2000. Tracking long-term changes in climate using algal indicators in lake sediments. J. Phycol. 36, 986–1011.
- Smol, J.P., Douglas, M.S., 2007. From controversy to consensus: making the case for recent climate change in the Arctic using lake sediments. Front. Ecol. Environ. 5, 466–474.
- Steinhilber, F., Beer, J., Frölich, C., 2009. Total solar irradiance during the Holocene. Geophys. Res. Lett. 36, L19704.
- Stuiver, M., Reimer, P.J., 1993. Extended 14C database and revised CALIB radiocarbon calibration program. Radiocarbon 35, 215—230.
- Thompson, R.S., Anderson, K.H., Bartlein, P.J., 1999. Atlas of Relations Between Climate Parameters and Distributions of Important Trees and Shrubs in North America Introduction and Conifers. U.S. Geological Survey, Denver, CO.
- Voigt, R., Grüger, E., Baier, J., Meischner, D., 2008. Seasonal variability of Holocene climate: a palaeolimnological study on varved sediments in Lake Jues (Harz Mountains, Germany). J. Paleolimnol. 40, 1021–1052.
- Wunsch, C., 2006. Abrupt climate change: an alternative view. Quat. Res. 65, 191–203. Yu, S.Y., Colman, S.M., Lowell, T.V., Milne, G.A., Fisher, T.G., Breckenridge, A., Boyd, M., Teller, J.T., 2010. Freshwater outburst from Lake Superior as a trigger for the cold event 9300 years ago. Science 328, 1262–1266.
- Zdanowicz, C.M., Zielinski, G.A., Germani, M.S., 1999. Mount Mazama eruption: calendrical age verified and atmospheric impact assessed. Geology 27, 621–624.